

**ELECTRONIC SUPPLEMENTAL
INFORMATION:
Stabilizing Effect of TMAO on Globular PNIPAM
States: Preferential Attraction Induces
Preferential Hydration**

Martin A. Schroer,^{*,†,‡,¶} Julian Michalowsky,[§] Birgit Fischer,^{||} Jens Smiatek,^{*,§}
and Gerhard Grübel^{†,‡}

[†]*Deutsches Elektronen-Synchrotron DESY, Notkestr. 85, 22607 Hamburg, Germany*

[‡]*The Hamburg Centre for Ultrafast Imaging (CUI), Luruper Chausee 149, 22761 Hamburg,
Germany*

[¶]*present address: European Molecular Biology Laboratory EMBL c/o DESY, Notkestr. 85,
22607 Hamburg, Germany*

[§]*Institut für Computerphysik, Universität Stuttgart, Allmandring 3, 70569 Stuttgart,
Germany*

^{||}*Institut für Physikalische Chemie, Universität Hamburg, Grindelallee 117, 20146
Hamburg, Germany*

E-mail: martin.schroer@embl-hamburg.de; smiatek@icp.uni-stuttgart.de

Details of the metadynamics simulations

We performed metadynamics simulations^{1,2} using the PLUMED 1.3 package³ at various temperatures between 295 K and 315 K with 5 K intervals. The length of a single metadynamics simulation was 50 ns with a timestep of 2 fs. As initial configuration, we used the energy-minimized structure of PNIPAM in pure water. All simulations were performed in NVT ensemble using the Berendsen thermostat⁴. The radius of gyration R_g of PNIPAM as defined by

$$R_g^2 = \frac{1}{N} \sum_{i,j}^N (\vec{r}_i - \vec{r}_j)^2 \quad (1)$$

with the positions of the C_α backbone carbon atoms was chosen as collective variable. The width and the height of the Gaussian hills were $\sigma = 0.1$ nm and $\omega = 0.1$ kJ/mol, respectively. New hills were deposited each 2 ps to ensure proper relaxation². A typical example for the trajectory in the monitored collective variable space R_g at 300 K is shown in Fig. 1. One can

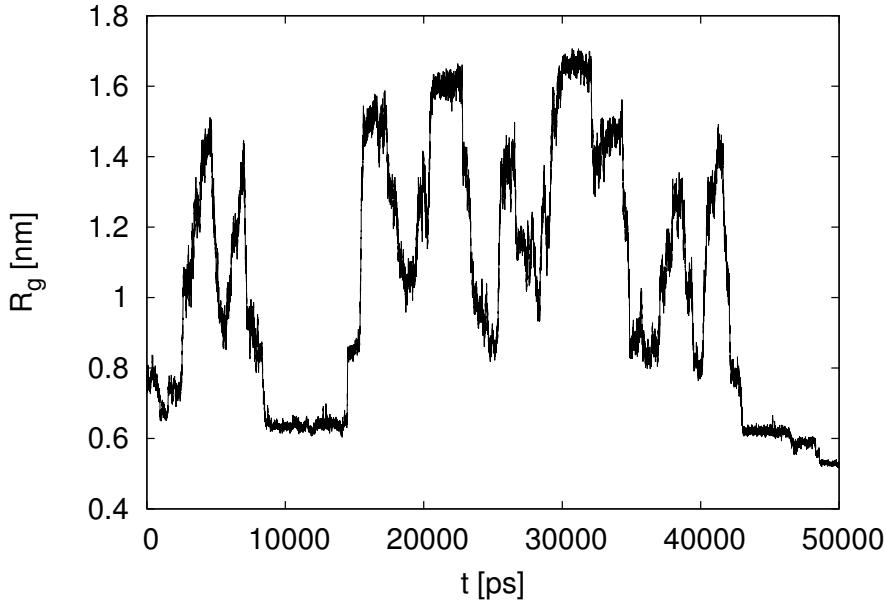


Figure 1: Trajectory of the metadynamics simulation in the monitored collective variable space R_g at 300 K.

clearly see, that often visited states belong to conformations with $R_g \approx 0.8$ nm and $R_g \approx 1.4$ nm, which were therefore chosen as reference states for our subsequent restrained position

simulations. The observation of higher or lower values of R_g is induced by the energy hill deposition procedure², inducing stronger and less relevant deformations of PNIPAM at the boundaries of the phase space. Therefore, we disregarded these conformations and concentrated on the more reliable conformations at the R_g positions mentioned above. Moreover, the back- and forward moving in phase space, which guarantees a full exploration of the accessible collective variable space is evident. As a side remark, the collective variable space was nearly comparable for all temperatures between 295 K and 315 K, assuming that the reference conformations can be regarded as representative conformations in this temperature range.

Cumulative number of molecules around PNIPAM

The cumulative number of molecules around PNIPAM can be calculated by Eqn. (9) in the main text. The exemplary results for water and TMAO molecules around a coil conformation of PNIPAM at 288 K are shown in Fig. 2.

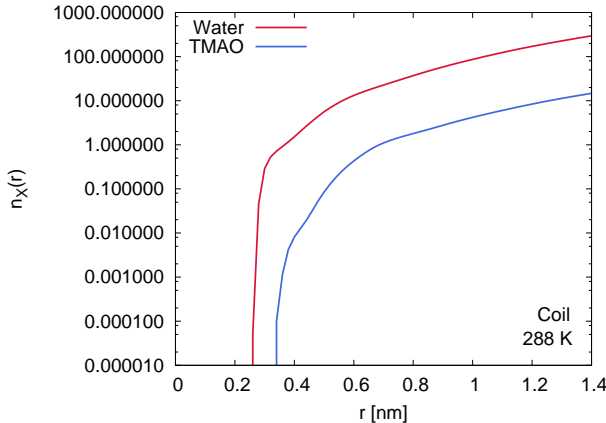


Figure 2: Cumulative number of molecules around a coil state of PNIPAM at 288 K for different distances r . The results for different PNIPAM configurations, different temperatures and different TMAO concentrations are comparable.

Transfer free energies and preferential binding parameters

Table 1: Preferential binding coefficients ν_{23} for TMAO and transfer free energies ΔF_{23} for the different PNIPAM conformations, TMAO concentrations c and temperatures T .

T [K]	Conformation	c [mol/L]	ν_{23}	ΔF_{23} [kJ/mol]
288	Coil	1.26	1.81	-4.33
288	Globule	1.26	5.56	-13.31
288	Coil	2.53	0.95	-2.27
288	Globule	2.53	4.17	-9.98
328	Coil	1.26	3.18	-7.61
328	Globule	1.26	6.07	-14.53
328	Coil	2.53	2.43	-5.82
328	Globule	2.53	6.87	-16.45

Local/bulk partition coefficients

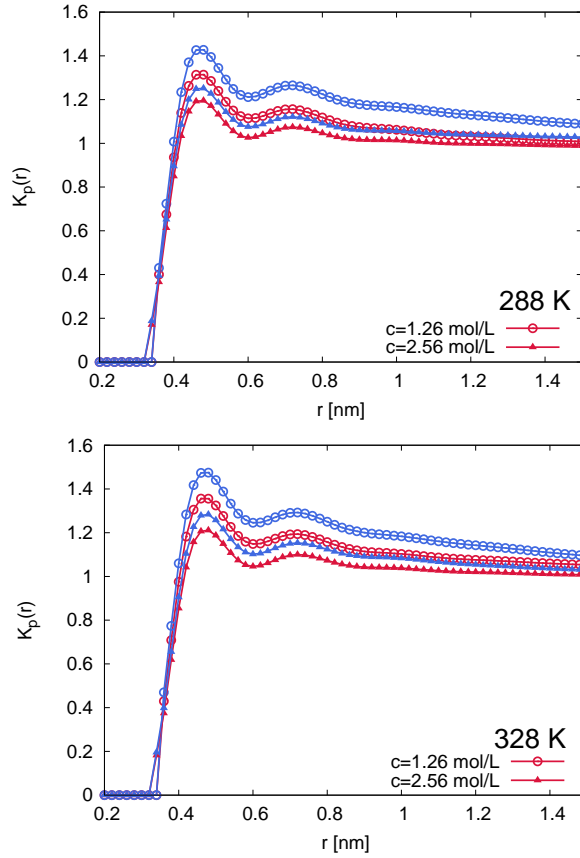


Figure 3: Local/bulk partition coefficients $K_p(r)$ for TMAO concentrations of $c = 1.26$ mol/L (circles) and $c = 2.56$ mol/L (triangles) around the globular (blue lines) and the coil conformation (red lines) at 288 K (top) and 328 K (bottom).

Differences in the transfer free energies

Table 2: Difference of the transfer free energies $\Delta\Delta F_{23}$ for the transition from the globular to the coil states for different TMAO concentrations and temperatures.

T [K]	c [mol/L]	$\Delta\Delta F_{23}$ [kJ/mol]
288	1.26	8.98
288	2.53	7.71
328	1.26	6.92
328	2.53	10.63

Hydrogen bond kinetics

In order to study the kinetics of the hydrogen bonds between PNIPAM and water molecules, we calculated the time-dependent rate constant⁵ as defined by

$$k(t) = -\frac{dc}{dt} = -k_c c(t) + k_n n(t) \quad (2)$$

where k_c and k_n denote the rate constants for the formation and cleavage of a hydrogen-bonded pair of molecules and $c(t)$ and $n(t)$ the corresponding probabilities. Thus, $k(t)$ can be interpreted as the relaxation rate towards equilibrium and hence, $-k(t)$ as the average rate of change of hydrogen bond population for a hydrogen-bonded pair of molecules. The corresponding results for both PNIPAM conformations and both TMAO concentrations at different temperatures are depicted in Fig. 4. For short times $t \leq 10$ ps, one can observe the largest values of $k(t)$ with the order $c = 2.53$ mol/L $<$ $c = 1.26$ mol/L $<$ $c = 0.0$ mol/L at $T = 328$ K whereas this trend is less pronounced for lower temperatures. Thus, at short times the presence of TMAO enhances the probability of hydrogen bonded PNIPAM-water pairs. In contrast, for longer times $t > 30$ ps the above mentioned order is reversed. However, the impact of this effect at longer times is less important due to the small values for $k(t) < 0.01$ ps⁻¹. In summary, TMAO induces a slight amplification of hydrogen bond occurrence probabilities at the more important short time scales and specifically at higher temperatures.

Structural properties of hydrogen bonds

In order to study the structural properties of hydrogen bonds, we first evaluated the angular distribution of hydrogen bonds between PNIPAM-water donor-acceptor pairs for different concentrations of TMAO, different coil and globular states of PNIPAM and at different temperatures. The results are shown in Fig. 5. It is evident that the presence of TMAO

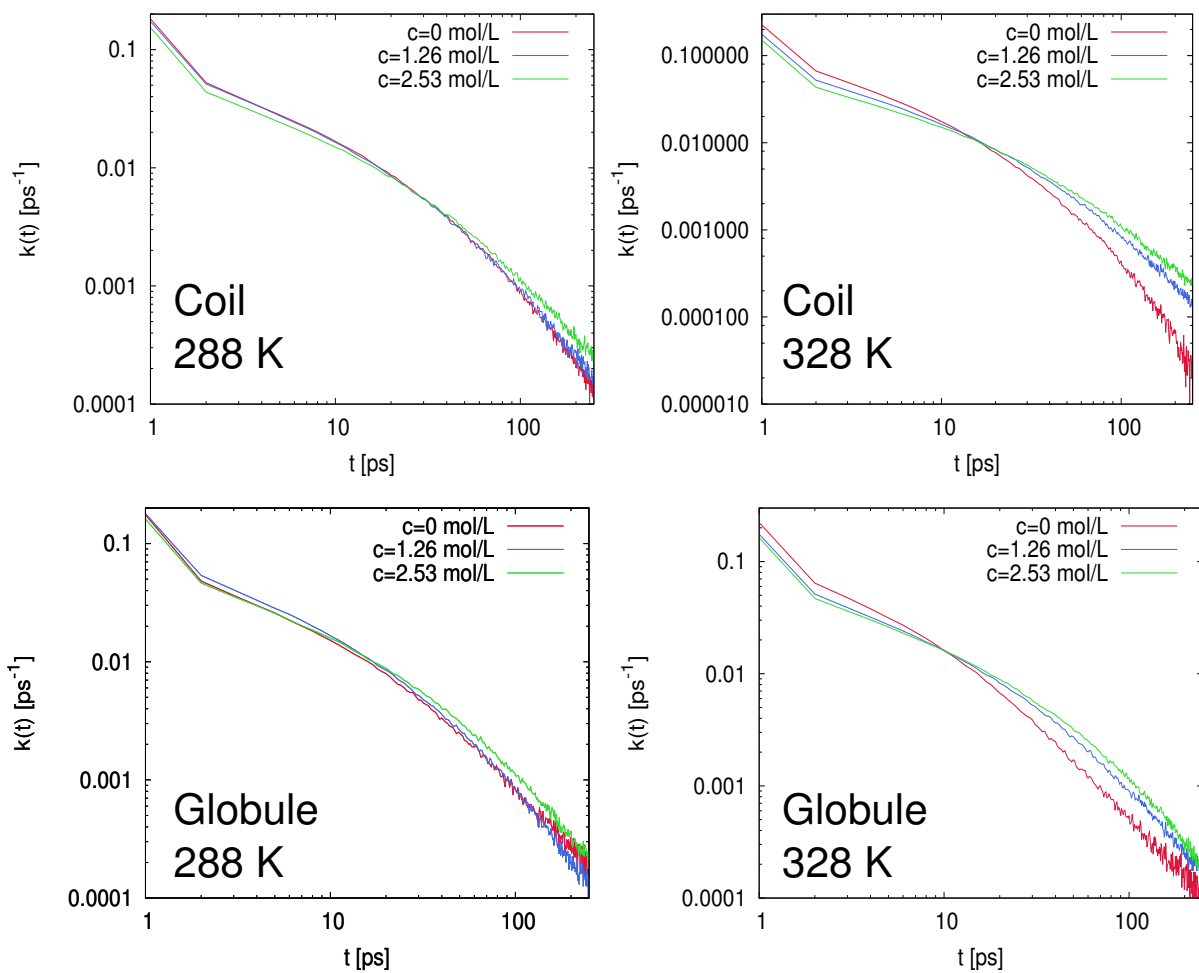


Figure 4: Time-dependent rate constant $k(t)$ for hydrogen bonds between PNIPAM and water molecules for TMAO concentrations $c = 1.26$ mol/L (blue line), $c = 2.53$ mol/L (green line) and without TMAO (red line) for coil and globular conformations of PNIPAM at different temperatures as denoted in the inset.

induces a higher ordering in the distribution of hydrogen bond angles. Thus, the distribution becomes more narrow and the fluctuations for the hydrogen bond angles in presence of TMAO are more restricted. The effects are more pronounced at higher temperatures. We also

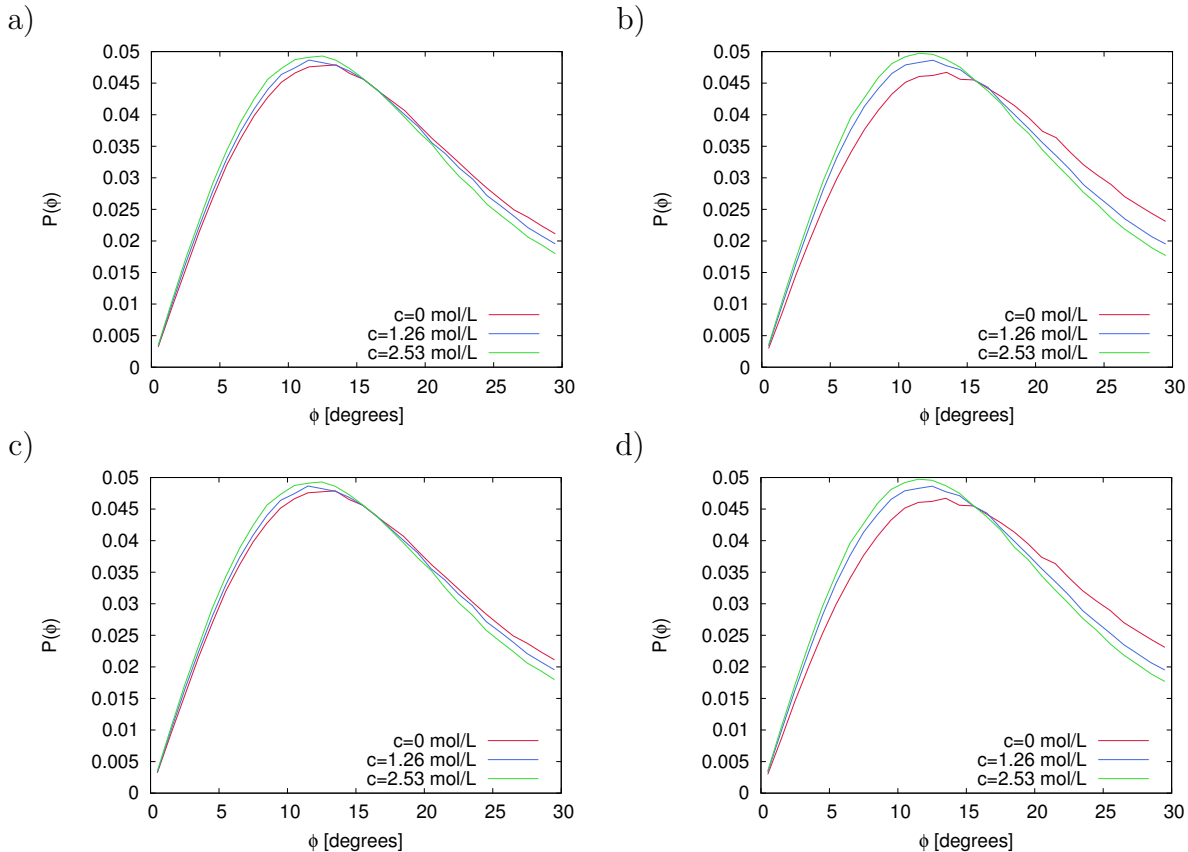


Figure 5: Angular distribution of hydrogen bonds between PNIPAM and water donor-acceptor pairs for different TMAO concentrations as denoted in the legend for a) coil state (PNIPAM), $T = 288$ K, b) coil state (PNIPAM), $T = 328$ K, c) globular state (PNIPAM), $T = 288$ K, d) a) globular state (PNIPAM), $T = 328$ K.

calculated the probability distribution for the PNIPAM-water donor-acceptor pair distance. The corresponding results are depicted in Fig. 6. The results are comparable to our findings for the angular distribution. At higher temperatures and in presence of TMAO, the distance distribution becomes more narrow and therefore fluctuations are more restricted. Nearly no effects were found at 288 K. Based on our findings, we can conclude that TMAO leads to a slight increase of hydrogen bond order and stability. The effects are more pronounced at higher temperatures.

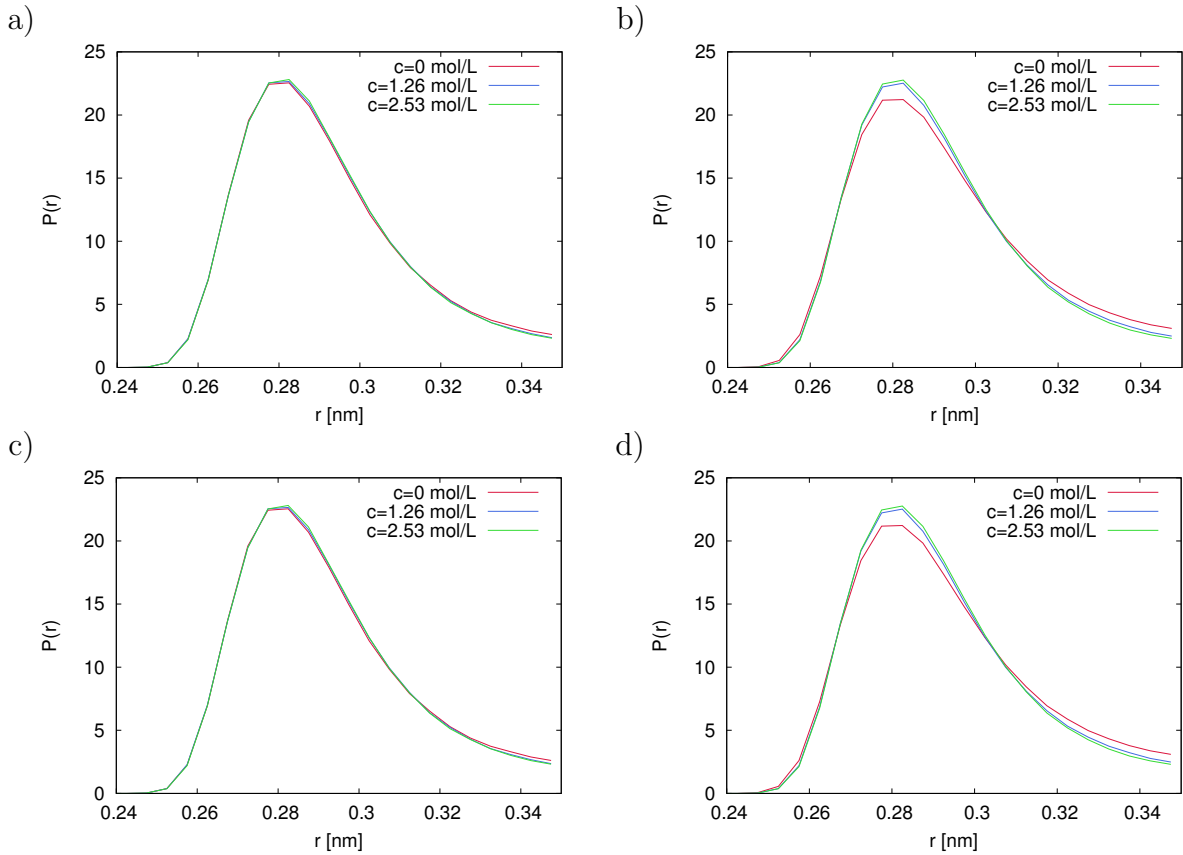


Figure 6: Distance distribution of hydrogen bonds for PNIPAM and water donor-acceptor pairs for different TMAO concentrations as denoted in the legend for a) coil state (PNIPAM), $T = 288$ K, b) coil state (PNIPAM), $T = 328$ K, c) globular state (PNIPAM), $T = 288$ K, d) a) globular state (PNIPAM), $T = 328$ K.

References

- (1) Laio, A.; Parrinello, M. *Proc. Natl. Acad. Sci. USA* **2002**, *99*, 12562–12566.
- (2) Laio, A.; Gervasio, F. L. *Rep. Prog. Phys.* **2008**, *71*, 126601.
- (3) Bonomi, M.; Branduardi, D.; Bussi, G.; Camilloni, C.; Provasi, D.; Raiteri, P.; Donadio, D.; Marinelli, F.; Pietrucci, F.; Broglia, R. A. *Comput. Phys. Commun.* **2009**, *180*, 1961–1972.
- (4) Berendsen, H. J.; Postma, J. P. M.; van Gunsteren, W. F.; DiNola, A.; Haak, J. J. *Chem. Phys.* **1984**, *81*, 3684–3690.
- (5) Luzar, A.; Chandler, D. *Nature* **1996**, *379*, 55–57.